Proceedings of ASME Turbo Expo 2008: Power for Land, Sea and Air
GT2008
June 9-13, 2008, Berlin, Germany

GT2008-50834

COMPUTATIONAL FLUID DYNAMIC PREDICTION OF NOISE FROM A COLD TURBULENT PROPANE JET

Tanya S. Stanko*
Centre for Computational Fluid Dynamics

Derek B. Ingham
Centre for Computational Fluid Dynamics

Michael Fairweather
Energy and Resources Research Institute

Mohamed Pourkashanian
Energy and Resources Research Institute

School of Process, Environmental and Materials Engineering,
University of Leeds, Leeds LS2 9JT, UK

ABSTRACT

Numerical solutions of a turbulent jet flow are used to provide velocity information throughout a simple cold turbulent propane jet at a Reynolds number of 68,000. Predictions provided by the Reynolds-averaged Navier-Stokes simulations, based on a Reynolds stress turbulence model, are compared with experimental data available in the literature. The effect of the modelled inlet boundary conditions on the predicted flow field is described, and the discrepancy between the simulation results and experiment measurements is found to be less than the corresponding variations due to uncertainness in the experimental boundary conditions. In addition, these solutions are used as the basis for noise predictions for the jet based on Lighthill's theory using the Goldstein broadband noise source formalization that postulates axisymmetric turbulence superposed on the mean flow. The latter model provides an aeroacoustic tool that is reasonable in identifying components or surfaces that generate significant amounts of noise, thereby providing opportunities for early design changes to aircraft and gas turbine components.

INTRODUCTION

Jet noise simulation has developed over the last decade with the aim of providing a better understanding of sound generation in turbulent flows. This work has generally involved complementary experimental and mathematical modelling studies, and has led to methods that are now able to reliable predict many practical flows. The most popular acoustic formulations, based on the general theory for flow noise of Lighthill [1, 2], are the specialized formulations for jet noise of Proudman [3], Lilley [4], Ribner [5] and Goldstein and Rosenbaum [6]. These specialized formulations provide a framework for estimating the source terms (via correlations) required by the general theory. Under certain simplifying assumptions, all specialized theories lead to analytical expressions which allow the prediction of the noise radiation from a relatively small number of local turbulent flow quantities.

The feasibility of computing jet noise directly by solving the unsteady, compressible Navier-Stokes equations has been demonstrated, for example, by Freund [7] and Bogey et al. [8]. Subsonic single unheated jets at low and moderate Reynolds numbers have been calculated by Direct Numerical Simulation (DNS) and Large Eddy Simulation (LES). However, the direct computation of the unsteady compressible Navier-Stokes equations is usually not a convenient approach for engineering problems. This is because it requires a substantial amount of computational time and resources.

In the present paper, the Broadband Noise Source (BNS) model, based on the Goldstein formalization (Goldstein and Rosenbaum [6]), is employed. BNS requires steady state flow solutions which are provided by Reynolds-averaged Navier-Stokes (RANS) computations based on a Reynolds stress turbulence model (Launder et al. [9]). RANS simulations are relatively inexpensive in terms of the computation time, as compared to DNS and LES, and consequently BNS models can be used on the basis of such simulations as effective and inexpensive design tools.

The purpose of this paper is to simulate numerically the noise generated by a cold propane turbulent jet at a Reynolds number of 68,000. The simulation results for the velocity and mixing fields are validated against the experimental data obtained by Schefer and Dibble [10] from the Sandia National Laboratory. Having obtained reasonable agreement between the simulated velocity field and the experimental data, it is reasonable to assume that the noise calculations based on the verified velocity field are valid. It is also of interest to investigate the noise level produced by the cold propane jet when the co-flow velocity used in the original experimental study is varied.

AEROACOUSTIC MODELLING

Aeroacoustic behavior can be completely characterized by solving the compressible Navier-Stokes equations. In other words, aeroacoustic phenomena can be explained through the use of the principles of mass, momentum, and energy conservation. For simple problems, Direct Numerical Simulations that solve the compressible Navier-Stokes equations are able to solve for both the aerodynamic flow field and the acoustic field. However, for problems in industrial applications, this approach becomes extremely difficult due to the fact that the acoustic energy is usually several orders of magnitude smaller than the hydrodynamic energy. In addition, the acoustic pressure perturbations are generally several orders of magnitude smaller than the hydrodynamic pressure. The length and time scales of the two fields are therefore not compatible, and the need to separate the two fields becomes apparent.

Theory of aerodynamic noise

It was Lighthill [1, 2] who founded the theory of aeroacoustic by rearranging the Navier-Stokes equations and deriving the well known wave equation, namely

$$\frac{\partial^2 \rho}{\partial t^2} - c_0^2 \nabla^2 \rho = \frac{\partial^2 T_{ij}}{\partial x_i \partial x_j} \tag{1a}$$

with

$$T_{ij} = \rho v_j v_j - \sigma_{ij} + (p - c_0^2 \rho)\delta_{ij} \tag{1b}$$

where T_{ij} is the so-called Lighthill turbulence stress tensor for the acoustic field, δ_{ij} is the Kronecker delta, which is 1 if $i = j$ and 0 otherwise, and c_0 is the speed of sound in the medium at rest.

Equation (1a) basically decouples the hydrodynamic field and the sound field and is the basis of Lighthill's acoustic analogy. As a result, the processes of noise generation and propagation can be separately addressed. The practical implications of this theory are significant since the propagation of sound waves amounts to solving a hyperbolic wave equation in a medium at rest with externally applied forces.

In 1952, Lighthill [1, 2] derived the sound propagation equation for unbounded flows. In 1955, Curle [11] added the effects of non-moving boundaries. In 1969, Ffowcs-Williams and Hawkings [12] derived a generalized form of Lighthill's equation with moving boundaries. The Ffowcs-Williams and Hawkings' equation can be used to solve a wave equation for the noise propagation in a medium at rest with applied monopole, dipole, and quadrupole sources. These applied external forces can in turn be obtained from a computational fluid dynamic (CFD) solver.

Broadband noise source models

Previous approaches have generally used a transient CFD solution that captures the flow structures and presents challenges in terms of resource requirements and computational time that are usually not acceptable for real industrial applications.

In practice, when the generated sound does not have any distinct tone and the radiated sound energy is distributed over the entire range of frequencies, statistical turbulence quantities extracted from steady state RANS solutions can be used, together with semi-empirical correlations, to provide a measure of the broadband source noise. Aeroacoustic models that quantify the broadband source noise generated by the flow per unit surface or volume are termed Broadband Noise Source (BNS) models. Though BNS models are attractive aeroacoustic tools, they have major limitations. These models do not, therefore, provide any tonal noise information or noise spectra at receiver locations. Instead, they provide only an approximate measure of the radiated noise at the source.

In this paper the Goldstein and Rosenbaum [6] acoustic formulation is applied. The Acoustic Power (AP) per unit volume of a turbulent jet is defined as

$$AP = 2\pi x^2 \int_0^{\pi} I(x, \vartheta / \vec{y}) \sin \vartheta d\vartheta \tag{2}$$

where x is an observation point in the far field (from Eq.(2) it follows that observation points are distributed throughout the space), ϑ is the angle between the direction of the mean flow and the direction of the observation point x, and $I(x, \vartheta / \vec{y})$ is the total directional acoustic intensity per unit volume of the jet, defined as the sum of a self-noise intensity component and a shear-noise intensity component:

$$I(x, \vartheta / \vec{y}) = I^{Se.N.}(x, \vartheta / \vec{y}) + I^{Sh.N.}(x, \vartheta / \vec{y}) \tag{3}$$

with the self-noise intensity is defined by

$$I^{Se.N.}(x,\vartheta/\vec{y}) = \rho_0 \frac{12 L_1 L_2^2}{5\pi c_0^5 x^2} \overline{u'^2} \omega_f^4 \frac{D_i^{Se.N.}}{C^5} \qquad (4a)$$

where

$$D_i^{Se.N.} = 1 + 2\left(\frac{M}{9} - N\right)\cos^2\vartheta \sin^2\vartheta + \\ + \frac{1}{3}\left[\frac{M^2}{7} + M - 1.5N\left(3 - 3N + \frac{1.5}{\Delta^2} - \frac{\Delta^2}{2}\right)\right]\sin^4\vartheta \qquad (4b)$$

The shear-noise intensity is defined by:

$$I^{Sh.N.}(x,\vartheta/\vec{y}) = \rho_0 \frac{24 L_1 L_2^4 \overline{u'^2}}{\pi c_0^5 x^2}\left(\frac{\partial \overline{U}}{\partial y_2}\right)^2 \omega_f^4 \frac{D_i^{Sh.N.}}{C^5} \qquad (5a)$$

where

$$D_i^{Sh.N.} = \cos^2\vartheta(\cos^2\vartheta + \frac{1}{2}\left[\frac{1}{\Delta^2} - 2N\right]\sin^2\vartheta) \qquad (5b)$$

In these expressions the effects of the anisotropic structure of the turbulence appear through the following parameters:

$$\Delta = \frac{L_2}{L_1},\ N = 1 - \frac{\overline{v'^2}}{\overline{u'^2}},\ M = \left[1.5\left(\Delta - \frac{1}{\Delta}\right)\right]^2,\ \omega_f = 2\pi\frac{\varepsilon}{k}$$

Here, ω_f is a typical angular frequency of the turbulence, L_1 and u'^2 (L_2 and v'^2) are the longitudinal (transversal) integral scales of the kinetic energy of the turbulence and the turbulent velocity fluctuations, respectively, which cab be defined from RANS calculations as follows: $L_1 = \left(\overline{u'^2}\right)^{3/2}/\varepsilon$ and $L_2 = \left(\overline{v'^2}\right)^{3/2}/\varepsilon$, where k is a turbulence kinetic energy and ε is a rate of dissipation in a k-ε RANS model. In the RSM model $u'^2 = 8/9\,k$ and $v'^2 = 4/9\,k$; $\overline{U}$ is the axial mean flow velocity and C is the convection factor, $C = 1 - M_c\cos\vartheta$, where M_c designates the convection Mach number.

All these parameters can be obtained directly from the steady Reynolds stress solution used in the present work, or alternatively from a *k*-ε RANS solution, as was done by Bechara et al. [13].

This paper is focused on simulating the noise generated by a propane jet issuing into air, where the density variations may have some contribution to the noise generation. Although the variation of the density is not explicitly included in the BNS model, the effect of the density change appears implicitly in the velocity variations.

In order to use Lighthill's equation to predict the sound intensity from the known properties of a turbulent shear flow, it is necessary to measure or deduce analytically the two-point space-time correlations of the second time derivatives of the Reynolds stresses and then integrate the results over the turbulent region. Goldstein and Rosenbaum [6] developed a model for predicting the jet noise based on the set of assumptions: (a) the eddy convection Mach number is small, (b) the turbulence is considered to be locally homogeneous so that it is possible to decompose the sound intensity into shear and self-noise components, (c) the joint probability distribution of the velocities at a fixed time is approximately normal, and (d) the turbulence in the jet is axisymmetric.

PROBLEM DESCRIPTION

Schefer and Dibble [10] examined a propane jet issuing from a circular pipe into co-flow of air. The fully-windowed test section of the experimental rig had a square cross-section and was 200 cm long. The fuel nozzle had an inside diameter of 0.526 cm and an outer diameter of 0.9 cm. The fuel jet (bulk) velocity was 53 m/s (± 0.1m/s) and the co-flow air velocity was 9.2 m/s (± 0.1m/s). Fig. 1 shows a schematic diagram of the Sandia experiment, where the origin of the coordinate system coincides with the centre of the nozzle outlet. The test section dimensions and the inlet conditions are summarized in Table 1.

Table 1. Test section dimensions and inlet conditions

Orientation	Vertical
Test section	30cm x 30cm
Jet tube exit	0.526 cm (inside ϕ) 0.900 cm (outside ϕ)
Length of fuel jet tube straight section	2m
Propane jet velocity	53 m/s (± 0.1 m/s)
Propane jet temperature	294 K (± 2K)
Co-flow air velocity	9.2 m/s (± 0.1 m/s)
Co-flow air temperature	294 K (± 2K)
Reynolds number based on jet exit ϕ	68,000
Co-flow air turbulence	0.4%
Axial pressure gradient	6 Pa/m

Velocity measurements at the test section inlet showed that the maximum velocity on the centreline of the jet was $u_{j,\max} = 69$ m/s, and this is consistent with fully-developed, turbulent pipe flow ($u_{j,\max} = 1.28u_{j,bulk}$). A thin boundary layer was also measured along the outer edge of the jet pipe with a thickness of approximately 0.3 jet diameters at the exit plane of the jet.

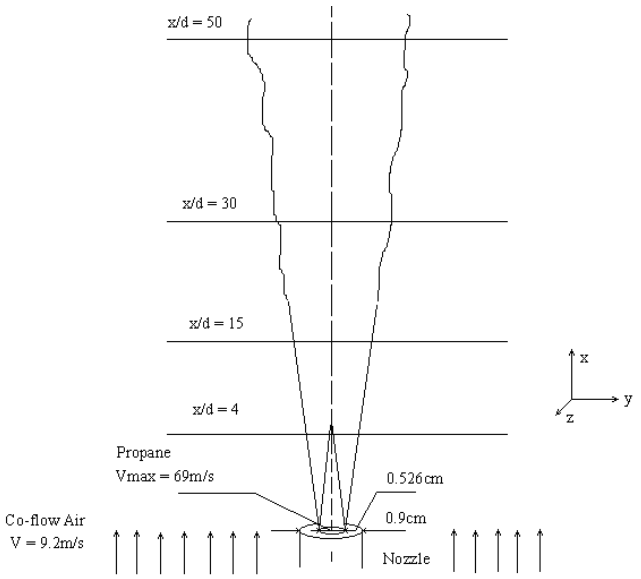

Figure 1. Schematic diagram of the Sandia experiment performed by Schefer and Dibble (2001)

The experimental data set, derived based on the conditions given in Table 1, includes the mean axial and radial velocity components, the r.m.s. of each fluctuating velocity component, the correlation between the axial and radial fluctuating velocities, and propane mass fraction measurements.

The measurements were made in the radial direction at downstream locations of x/d = 4, 15, 30 and 50, and in the axial direction along the jet axis (y/d = 0), as shown in Fig. 1. The velocity measurements were made using a two-colour Laser Doppler Velocimetry (LDV) system. In the data analysis, it was assumed that the seed particles (0.85 μ m diameter) employed followed the motion of the fluid, and that the difference between the diffusivity of the particle and the fluid was negligible. Seeding was added alternately into the jet or into the co-flowing air stream, giving different values for the velocity components of the flow. In the present work, velocities obtained by seeding the main jet flow are used for comparison purposes.

COMPUTATIONAL DETAILS

The natural symmetry of the problem allows consideration of a two-dimensional, axisymmetric flow, rather than having to consider the full three-dimensional flow case. The computational domain for the simulation of the jet flow was therefore 2D axisymmetric, with dimensions (43 cm × 15 cm), as shown in Fig. 2.

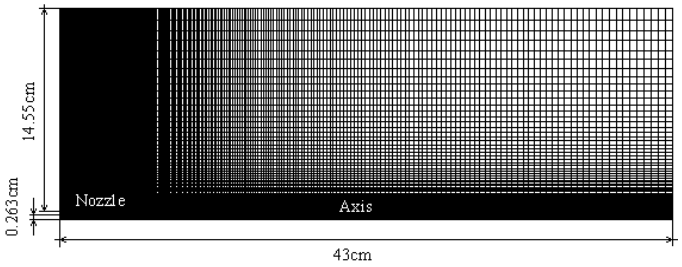

Figure 2. Diagram showing the computational mesh and domain

After a set of sample runs, where the mesh resolution was varied, the operational grid, which gave results free on numerical error, consisted of 60 k nodes, whis 50 nodes equally distributed along the inner radius of the nozzle, 25 nodes equally distributed along the edge of the nozzle, and 80 nodes used along the edge of the domain starting from the outer wall of the nozzle up to the end of the domain, with an expansion ratio of 1.05. 400 nodes were used along the axis of the jet for a distance 43 cm, with an expansion ratio of 1.01.

FLOW FIELD RESULTS AND DISCUSSION

The jet flow simulation results are validated with respect to the Schefer and Dibble [10] measurements for the mean velocity, ($\overline{U}$), r.m.s. fluctuating velocity components ($\sqrt{u'^2}$ and $\sqrt{v'^2}$), their correlation ($\overline{u'v'}$), and mixture fraction ($\overline{f}$), as shown in Fig. 3.

Since the initial velocity profile for the jet flow is unknown from the experiment, it has to be prescribed. Two different initial velocity profiles for the jet were applied in the simulations, namely: a flat velocity profile and the theoretical prediction for the velocity profile of a fully developed turbulent flow in a tube, derived by Prandtl, see Tietjens [14]. The Prandtl velocity profile is defined as:

$$\frac{U}{U_{\max}} = \left(1 - \frac{y}{0.5d}\right)^{1/7} \tag{6}$$

where d is the diameter of the pipe, $U_{\max}$ = 69 m/s is the maximum velocity at the outlet of the pipe, and U is the local velocity at a radial distance y. The details of the simulations are summarised in Table 2.

Different turbulence models were studied in the current work, although the Reynolds stress turbulence model was found to be the most appropriate for the propane jet simulations. Therefore, only results obtained using this model are presented here.

Table 2. Details of the jet flow simulation

Material	Mixture: propane-air obeying ideal gas law
Turbulence model	Reynolds Stress Model
Propane inlet Mass flux ($V\rho$)	Flat profile or Prandtl profile, T = 294K Turbulence intensity: 4% Hydraulic diameter: 0.263 cm
Air inlet Mass flux ($V\rho$)	Flat profile $11.27\ kg/m^2s$ T = 294K Turbulence intensity: 0.4% Hydraulic diameter: 14.55 cm
Outlet	Pressure outlet = P atm T = 294K
Solver	Axisymmetric, Pressure Based Implicit, Steady

Reasonably good agreement between velocity measurements and predictions is observed, and this is in general true for both types of inlet velocity profiles employed. However, the simulations based on the analytically derived Prandtl velocity profile at the inlet tend to predict better the flow behaviour in the initial part of the jet than at the simulations with a flat velocity profile at the inlet, as shown in Fig. 3 (a, b), (e, f), (i, j), and (m, n).

In addition, the simulation results for the mean mass fraction of propane are compared against experimental data in Fig.4, with good agreement again being found.

The close agreement between the CFD predictions and the experimental measurements, which is comparable to that obtained by Alvani and Fairwather [15] using a different RANS approach, indicates that the CFD model is capable of predicting the main physical characteristics of the flow reasonably well. Therefore we conclude that the simulation results appear sufficiently reliable to be used as a basis for noise predictions.

ACOUSTIC RESULTS AND DISCUSSION

The Broadband Noise Source model, using Goldstein's jet noise modification and the turbulence characteristics of the flow from CFD (discussed above), is employed to calculate an approximate measure of the total radiated noise.

Goldstein's acoustic model is available in FLUENT 6.3 [16], which in this work was used for both the flow field and noise predictions. FLUENT reports the acoustic power in dB computed by

$$L_p = 10\log\left(\frac{AP}{P_{ref}}\right) \tag{7}$$

where AP is the acoustic power per unit volume defined by Eq. (2) and P_{ref} is the reference acoustic power, $10^{-12}\ W/m^3$. Fig. 5 illustrates the simulation results for the jet acoustic power level in dB, calculated along the jet axis, for the two types of inlet velocity profiles: a flat velocity profile and the Prandtl velocity profile. A very small discrepancy in the two sets of simulation results is observed. Therefore, it can be concluded that the noise level generated by the jet does not in general depend on the type of the initially prescribed velocity profile, and consequently simple flat profiles could, in this case, be used as the basis of jet noise simulations.

The total noise generated by a jet is defined as the sum of the two components corresponding to Eq. (3). The self-noise component, $I^{Se.N.}(x, \vartheta/\vec{y})$, in the Goldstein model is defined by Eqs. (4a) and (4b), and depends mainly on the turbulence kinetic energy of the jet, while the shear-noise component, $I^{Sh.N.}(x, \vartheta/\vec{y})$, is defined by Eqs. (5a) and (5b), and depends on the turbulence kinetic energy as well as on the mean axial velocity of the jet.

To study the influence of the shear-noise component we may vary the parameter $U_{co-flowt}/U_{jet}$, where U_{jet} is the maximum inlet velocity of the propane jet, and $U_{co-flow}$ is the initial velocity of the co-flow air. In this work we have kept the U_{jet} constant.

Schefer and Dibble [10] used a co-flow/jet velocity ratio equal to 0.13. In this work, this ratio was varied between 0.06 and 0.27, i.e. having the velocity of the co-flow air $U_{co-flowt}/U_{jet}$, doubled or halved.

The numerical simulations for the three cases with a different co-flow/jet velocity ratios were performed with a flat velocity profile as the inlet boundary condition. This approach was used because the shape of the inlet velocity profile did not significantly change the maximum noise level or the position of the noise peak, as shown in Fig. 5. The numerical results for the noise generated by the jet with three values of $U_{co-flowt}/U_{jet}$ are shown in Fig. 6

The results shown in Fig. 6 demonstrate that noise is suppressed when the co-flow velocity is increased due to reduced shear between the jet and the co-flow [17]. This behaviour is in qualitative agreement with the experimental investigations performed, for example, by Papamoschou [17].

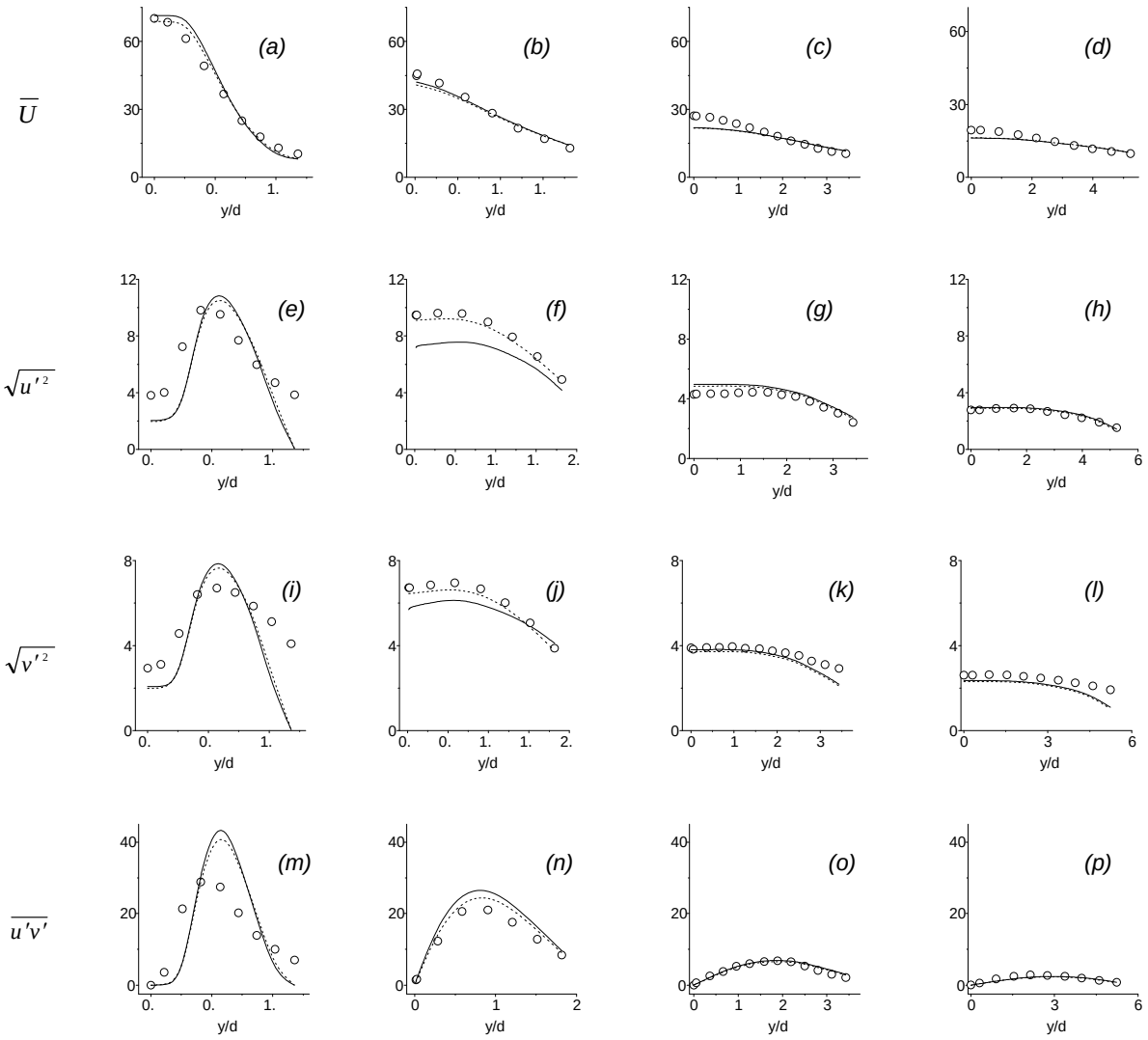

Figure 3. Radial direction profiles of the mean axial velocity component, fluctuating velocity components and their correlation, at x/d = 4 (a, e, i, and m); x/d = 15 (b, f, j, and n); x/d = 30 (c, g, k, and o); and x/d = 50 (d, h, l, and p). Legend: symbols - experimental data from Shefer and Dibble [10]; solid lines - simulation results with flat velocity profile at inlet; dashed line - simulation results with Prandtl velocity profile at inlet

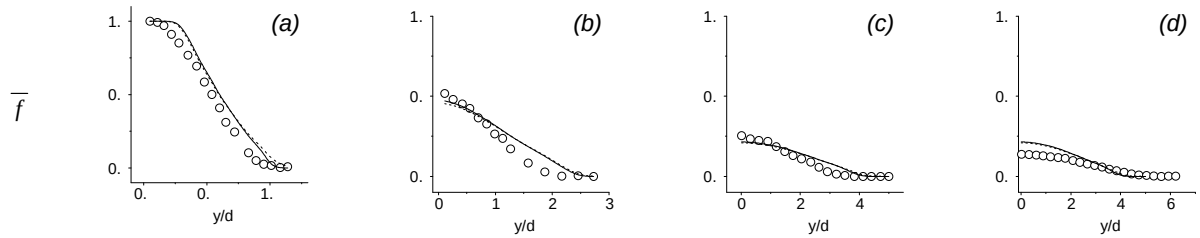

Figure 4. Radial direction profiles of the mean mixture fraction at x/d = 4 (a), 15 (b), 30 (c), and 50 (d). Legend: symbols - experimental data from Shefer and Dibble [10]; solid lines - simulation results with flat velocity profile at inlet; dashed line - simulation results with Prandtl velocity profile at inlet.

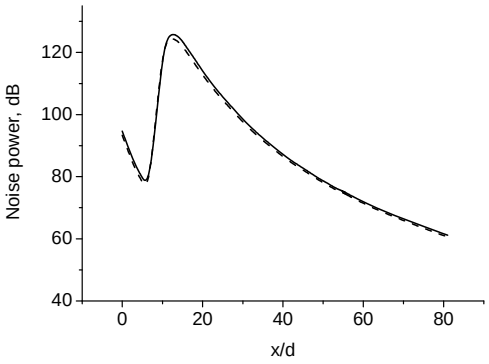

Figure 5. Jet acoustic power level along the axis of the jet: solid lines - simulation results with flat velocity profile at inlet; dashed line - simulation results with Prandtl velocity profile at inlet.

Papamoschou [17] showed that the noise level is suppressed when the velocity ratio, $U_{co-flow}/U_{jet}$, varies from 0 to 0.53, where the jet velocity, U_{jet}, is fixed, and the noise level is increased when the velocity ratio varies from 0.69 to 1. In the present research the velocity ratio, $U_{co-flow}/U_{jet}$, changes from approximately 0.06 to approximately 0.27. Therefore it is captured in the velocity range from 0 to 0.53 in Papamoschou's experimental work which shows that the noise level is suppressed when the co-flow velocity is increased.

It is observed in Fig. 6(a) that the maximum peak noise power is suppressed by approximately 4dB as the co-flow/jet velocity ratio is doubled, and it is increased by approximately the same amount when the co-flow/jet velocity ratio is halved, as shown in Fig. 7. Further Fig. 7 illustrates an almost linear dependency of the noise power on the co-flow velocity, which is not generally found to be the case [17]. However, the velocity ratio range investigated in this paper is relatively small, and therefore the linear behaviour observed is possibly a consequence of this phenomena.

CONCLUSIONS

Numerical solutions of a turbulent propane jet flow have been reported, and the predictions of the velocity, Fig.3, and mixing fields, Fig.4, within the jet have been demonstrated to be in reasonable agreement with the experimental data available in the literature. These predictions were subsequently used to predict noise levels within the jet, based on Lighthill's theory using the Goldstein broadband noise source formalisation. Results obtained using different jet exit to co-flow velocity ratios demonstrate that decreasing the velocity difference between the two flows reduces noise levels, as might be anticipated due to the reduced shear, and in qualitative agreement with the available data for the velocity ratios examined.

In the absence of noise data for this flow, future work will explore the use of LES to provide flow field information, and contrast noise results based on RANS and LES formulations with a view to assessing the likely accuracy of RANS-based approaches. Different, and more complex, aeroacoustic models will also be assessed.

Other ongoing work concerns the application of both RANS and LES approaches, coupled to various aeroacoustic models, to more complex flow geometries where noise data are available. The ultimate aim of this work is to provide validated flow and aeroacoustic models that can be used in the design of aircraft and gas turbine components

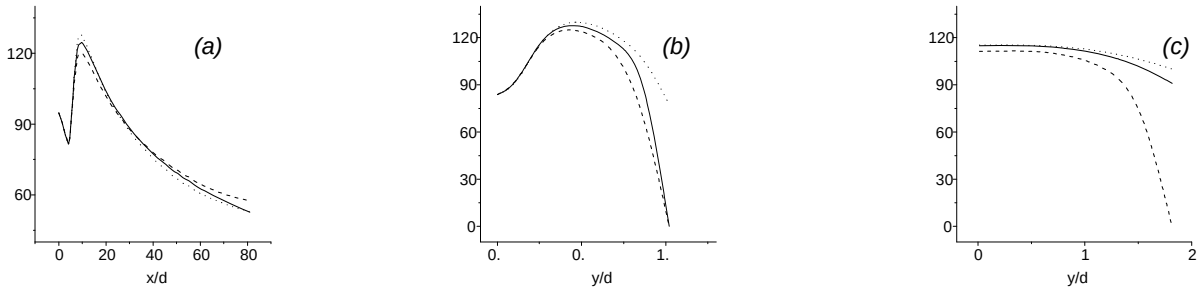

Figure 6. Jet acoustic power level (dB) predictions along the axis (a), and at the radial sections at the distance x/d = 4 (b) and 15 (c). Legend: solid lines - simulation results for a basic jet, $U_{co-flowt}/U_{jet}$ = 0.13; dashed lines - simulation results with a doubled co-flow velocity, $U_{co-flowt}/U_{jet}$ = 0.27; dotted lines - simulation results with a halved co-flow velocity, $U_{co-flowt}/U_{jet}$ = 0.06.

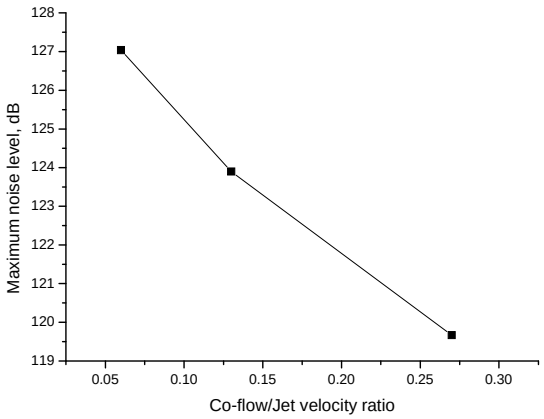

Figure 7. Simulation results of the maximum noise power level, in dB, predicted along the jet axis for three values of the jet/co-flow velocity ratio.

ACKNOWLEDGEMENT

The European Commission is gratefully acknowledged for the financial support of T.S. Stanko with an EST Marie Curie Fellowship, contract number MEST-CT-2005-020327.

REFERENCES

[1] Lighthill, M.J., 1952, "On sound generated aerodynamically - Part I. General theory", *Proc. R. Soc. London Ser. A*, Vol. **211**, pp. 564-587.

[2] Lighthill, M.J., 1954, "On sound generated aerodynamically - Part II. Turbulence as a source of sound", *Proc. R. Soc. London Ser. A*, Vol. **222**, pp. 1-32.

[3] Proudman, I., 1952, "The generation of sound by isotropic turbulense", *Proc. R. Soc. London Ser. A*, Vol. **214**, pp. 119-132

[4] Lilley, G.M., 1958, "On the noise from air jets", *Aeronaut. Res. Council ARC*, pp. 20-376.

[5] Ribner, H.S., 1964, "The generation of sound by turbulent jets", *Adv. Applied Mechanics*, Vol. **8**, pp. 103-182.

[6] Goldstein, M.E., and Rosenbaum, B., 1973, "Effect of anisotropic turbulence on aerodynamic noise", *J. Acoust. Soc. Am.*, Vol. **54**, pp. 630-645.

[7] Freund, J.B., 2001, "Noise sources in a low-Reynolds-number turbulent jet at Mach 0.9", *J. Fluid Mech.*, Vol. **438**, pp. 277-30.

[8] Bogey, C., Bailly, C., and Juve, D., 2003, "Noise investigation of a high subsonic, moderate Reynolds number jet using a compressible LES", *Theoret. Comput. Fluid Dynamics*, Vol. **16**, pp. 273-297.

[9] Launder, B.E., Reece, G.J., and Rodi, W., 1975, "Progress in the development of a Reynolds-Stress turbulence closure", *J. Fluid Mech.*, Vol. **68**, pp. 537-566.

[10] Schefer, R.W., and Dibble, R.W., 2001, "Mixture fraction field in a turbulent non-reacting propane jet", *AIAA J.*, Vol. **39**, pp. 64-72.

[11] Curle, N., 1955, "The influence of solid boundaries upon aerodynamic sound", *Proc. R. Soc. A*, Vol. **231**, pp. 505-514.

[12] Ffowcs Williams, E.J., and Hawkings, D.L., 1969, "Sound generation by turbulence and surfaces in arbitrary motion", *Phil. Trans. R. Soc. A* , Vol. **264**, pp. 321-243.

[13] Bechara, W., Lafon, P., and Bailly, C., 1995, "Application of k-ε turbulence model to the prediction of noise for simple and coaxial free jets", *J. Acoust. Soc. Am.*, Vol. **97**, pp. 3518-3531.

[14] Tietjens, O.G., 1934, *Applied Hydro- and Aeromechanics: Based on Lectures of L. Prandtl*, McGraw-Hill, New York.

[15] Alvani, R.F., and Fairweather, M., 2008, "Prediction of the ignition characteristics of flammable jets using intermittency-based turbulence models and a prescribed pdf approach", *Computers & Chem. Eng.*, Vol. **32**, pp. 371-381.

[16] Fluent 6.3 Users Guide, 2007, *Fluent Inc., Lebanon NH*.

[17] Papamoschou, D., "Small-aperture phased array study of noise from coaxial jets", *Proceedings of the 45th AIAA Conference*, Reno, Nevada, USA (January 2007).